This is a previous version of the article published in Applied Catalysis B: Environmental. 2015, 174-175: 60-66. doi:10.1016/j.apcatb.2015.02.036

Active Oxygen by Ce-Pr Mixed Oxide Nanoparticles Outperform Diesel Soot Combustion Pt Catalysts

*Noelia Guillén-Hurtado, Avelina García-García, Agustín Bueno-López**

Department of Inorganic Chemistry; University of Alicante
Carretera de San Vicente s/n 03690. San Vicente del Raspeig – Alicante (Spain)
Fax: (+34) 965 90 3454
*Corresponding author: agus@ua.es

Abstract:

A $Ce_{0.5}Pr_{0.5}O_2$ mixed oxide has been prepared with the highest surface area and smallest particle size ever reported (125 m^2/g and 7 nm respectively), also being the most active diesel soot combustion catalyst ever tested under realistic conditions if catalysts forming highly volatile species are ruled out. This Ce-Pr mixed oxide is even more active than a reference platinum-based commercial catalyst. This study provides an example of the efficient participation of oxygen species released by a ceria catalyst in a heterogeneous catalysis reaction where both the catalyst and one of the reactants (soot) are solids. It has been concluded that both the ceria-based catalyst composition (nature and amount of dopant) and the particle size play key roles in the combustion of soot through the active oxygen-based mechanism. The composition determines the production of active oxygen and the particle size the transfer of such active oxygen species from catalyst to soot.

Keywords: Nanoparticles; Radicals; Ceria; Soot; Active oxygen

1.- Introduction

A typical heterogeneous catalysis reaction consists of a liquid or gas effluent whose molecules are adsorbed and react on the surface of a solid catalyst. The rate limiting step of this type of reactions can be either a chemical process occurring on the catalyst surface, the diffusion of the reactant molecules from the effluent bulk to the catalyst active sites or the release and diffusion of the reaction products from the catalyst surface back to the effluent bulk.

The combustion of diesel soot (solid carbon particles) accelerated by a solid catalyst can be considered, in somehow, a heterogeneous catalysis reaction, because the oxidizing species (mainly O_2 and NOx) are gases. However, it has the particular feature that one of the reactants, the soot carbon particles, is in solid state. This hinders significantly the performance of a solid catalyst due to the poor contact between the solid particles of soot and catalyst. In this reaction, the rate limiting step can additionally be the transfer of reaction intermediates from the catalyst surface to the soot particles, which in a real application is often restricted to the few contact points existing between soot and catalyst particles.

Important research efforts have been done during the last years in order to develop a suitable soot removal system for diesel vehicles [1, 2], because diesel soot is responsible of severe environmental and health problems [3, 4]. Typically, soot particles are collected in a filter placed in the exhaust pipe, and a catalyst is used in most cases to lower the soot combustion temperature [5, 6]. In order to solve the problem of the poor soot-catalyst contact, several strategies have been proposed. One of them consists of the impregnation of a low melting temperature catalyst, like a eutectic salt mixture ($Cs_2SO_4 \cdot V_2O_5$, for instance [7]) or an alkali compound (a potassium salt, for instance

[8]) into the filter. This type of catalysts melt under reaction conditions, and once in liquid phase, the contact with the soot particles is significantly improved. Unfortunately, these catalysts are progressively evaporated and have no practical relevance. Some other highly active catalysts, like those of ruthenium, iridium or osmium have neither practical interest because of the formation of volatile oxides [9, 10].

An elegant solution was found by Johnson Matthey, which is currently commercially available for heavy duty diesel vehicles like trucks and buses [11]. This system consists of a platinum-containing oxidation catalyst located upstream the soot filter. The platinum catalyst oxidizes the NO emitted by the engine to NO_2, which is much more oxidizing than NO and O_2 and initiates the oxidation of the soot collected downstream. This approach solves the problem of the poor soot-catalyst contact by using the high oxidation capacity of NO_2 [11].

Platinum catalysts are the most active ones for diesel soot oxidation in real conditions so far, but some other solid catalysts are being investigated to improve the activity and lower the price. Doped cerium oxides, and Ce-Pr mixed oxides in particular, are among the most promising candidates to replace platinum, because they are able to produce highly oxidizing active oxygen species [12-16]. This highly reactive active oxygen is produced by oxygen exchange between the cerium oxide-based catalyst and the oxygen-containing gas molecules (mainly O_2) [17]. In spite of this active oxygen-based reaction mechanism is well understood and that active oxygen species are expected to be much more oxidizing than NO_2, better soot combustion capacity than that of commercial platinum-based catalysts has not been reported so far. The main handicap of this highly efficient active oxygen-based reaction mechanism is the poor soot-catalyst contact, since most active oxygen species, which are postulated to be

oxygen radicals, recombine rapidly to each other and yield O_2 again before they reach the carbon surface.

In this study, Pr or Zr doped ceria catalysts of several compositions have been prepared by different methods, and soot combustion experiments have been performed with soot and catalyst solid particles mixed in the so-called “loose contact” mode [18]. It is mandatory to perform the experiments under realistic reaction conditions – gas mixture with both NOx and O_2 and poor soot-catalyst contact - in order to obtain results with practical relevance.

2.- Experimental details

2.1. Catalysts used

Two commercial catalysts were used as reference materials. A 1 wt. % Pt/Al_2O_3 catalyst was supplied by Sigma-Aldrich (BET surface area 160 m^2/g) and a $Ce_{0.8}Zr_{0.2}O_2$ catalyst was supplied by Rhodia and was used after calcination at either 500 or 800 ºC.

$Ce_xPr_{1-x}O_2$ (x = 0.8 or 0.5) and $Ce_{0.8}Zr_{0.2}O_2$ mixed oxides were prepared by reversed microemulsion, and the Pr and Zr loading was the optimum for this application according to previous studies (20 molar % for zirconium [19] and 50 molar % for praseodymium [14]). Reference catalysts were also prepared by coprecipitation with the same composition than those prepared by microemulsion and, for few selected compositions, mixed oxides were also prepared by nitrates calcination.

The Ce-Pr mixed oxides were prepared with the 3+ cation precursors $Ce(NO_3)_3{\cdot}6H_2O$ (Aldrich, 99.99%) and $Pr(NO_3)_3{\cdot}6H_2O$ (Aldrich, 99.9%) and the Ce-Zr mixed oxides with the 4+ cation precursors $(NH_4)_2Ce(NO_3)_6$ (Panreac, 99.0%) and

100 $ZrO(NO_3)_2 \cdot H_2O$ (Aldrich, x ≈ 6, technical grade). The selection of cation precursors of
101 similar charge favors homogeneous coprecipitation [20].

102 Catalysts preparation by reversed microemulsion method consisted of dissolving the
103 required amounts of each precursor in water, and a microemulsion in n-heptane was
104 prepared including Triton X-100 surfactant (polioxiethylene (9) 4 –(1,1,3,3,-
105 tetramethybutyl) phenyl ether) and hexanol as co-surfactant. For instance, in a typical
106 synthesis of 2 g of $Ce_{0.5}Pr_{0.5}O_2$, 2.6 g of the Ce precursor + 2.6 g of the Pr precursor
107 were dissolved in 20 ml of water, and 114 g of n-heptane, 37 g of Triton X-100 and 29 g
108 of hexanol were used. A similar microemulsion was prepared but with
109 tetramethylammonium hydroxide (6.8 g for a typical synthesis of 2 g of catalysts)
110 instead of the metal precursors. Both microemulsions were mixed and vigorously stirred
111 for 24 hours and, after precipitation, were centrifuged at 3000 rev/min for 6 minutes and
112 the liquid phases were decanted. The solids obtained were washed with ethanol, dried at
113 110 ºC and calcined at 500 ºC for 1 h.

114 Catalysts were prepared by coprecipitation by dissolving the required amounts of
115 each precursor in water, and ammonia was added drop wise until the precipitation was
116 complete (pH~9). The solids obtained were filtered, washed with deionized water, dried
117 in an oven at 110 ºC and calcined at 500 ºC for 1 h.

118 Finally, a selected a $Ce_{0.5}Pr_{0.5}O_2$ catalyst was prepared by calcination of an intimate
119 mixture of the metal precursors at 500 ºC for 1 h.

120 Table 1 includes details about the synthesis and characterization of all catalysts
121 prepared in this study.

122

123 *2.2. Catalysts characterization.*

124 Powder XRD patterns were recorded in a Bruker D8 advance diffractrometer,
125 using CuKα radiation. Diffractograms were registered between 10 and 60° (2θ) with a
126 step of 0.02º and a time per step of 3 s.

127 N_2 adsorption isotherms were obtained at -196 ºC in an automatic volumetric
128 system (Autosorb-6, Quantachrome). The catalysts were degassed at 250 ºC for 4 hours
129 under vacuum before the adsorption measurements. The BET surface areas were
130 determined and the particle sizes were estimated from the BET surface area values
131 assuming spherical shape of the particles and a density of 7.135 g/cm^3.

132 Raman spectra were recorded in a Bruker RFS 100/S Fourier Transform Raman
133 Spectrometer with a variable power Nd:YAG laser source (1064 nm). 64 scans at 85
134 mW laser power (70 mW on the sample) were recorded and no heating of the sample
135 was observed under these conditions.

136 Temperature Programmed Reductions with H_2 (H2-TPR) were carried out in a
137 Micromeritics Pulse ChemiSorb 2705 device, consisting of a tubular quartz reactor
138 coupled to a TCD detector. The reducing gas used was 5% H_2 in Ar, with a flow rate of
139 35 ml/min. The temperature range explored was from room temperature to 1000 ºC at a
140 heating rate of 10 ºC/min. Before the reduction, the catalysts were pretreated in situ at
141 500 ºC for 1 h with a gas flow of 5% O_2/He.

142 *2.3. Catalytic tests.*

143 Catalytic tests were performed in a tubular quartz reactor coupled to specific
144 NDIR-UV gas analyzers for CO, CO_2, NO, NO_2 and O_2 monitoring. 20 mg of soot and
145 80 mg of the selected catalyst were mixed in the so-called loose contact conditions and

diluted with SiC to avoid pressure drop and favor heat transfer. The model soot used in this study is a carbon black by Evonik-Degussa GmbH (Printex U). The gas mixture used contained either 500 ppm NOx/5% O_2/N_2 or 5%O_2/N_2, and the gas flow was fixed at 500 ml/min (GHSV = 30000 h^{-1}). Temperature Programmed reactions from room temperature until 700 ºC at 10 ºC/min were carried out. Blank experiments were also conducted under NOx/O_2 only with the catalysts (no soot), in order to analyze the NO_2 production capacity of the oxides.

3.- Results and discussion.

3.1. Catalysts characterization.

The catalysts were characterized by XRD and all catalysts showed the typical fluorite structure of ceria-based oxides. The X-ray diffractograms are not shown for the sake of brevity. The cell parameters and crystal sizes were determined with the (111) peak and the values obtained are compiled in Table 1. All ceria-based catalysts prepared present particle sizes between 6 and 31 nm, which were calculated from the N_2 adsorption isotherms. The smallest particles and the highest BET surface areas were obtained by the microemulsion method, and the values reached by $Ce_{0.5}Pr_{0.5}O_2$ are the highest ever reported for this material (more details and references are included below).

The cell parameters obtained for Zr-containing ceria catalysts are lower than the typical value assigned to pure ceria (~0.5424 nm), which is consistent with the substitution of the parent Ce^{4+} cations (0.097 nm) by smaller Zr^{4+} cations (0.084 nm). On the contrary, the cell parameters obtained with the Pr-containing ceria catalysts are equal or higher to the pure ceria value, because the size of Ce^{4+}/Ce^{3+} and Pr^{4+}/Pr^{3+} cations (0.097/0.114 and 0.096/0.113 nm, respectively) is almost equal. The higher cell

169 parameters obtained in some cases upon Pr doping must be attributed to the presence of
170 more 3+ cations, since Pr^{4+} is reduced more easily than Ce^{4+}.

171 These features of the ceria-based catalysts are confirmed by Raman
172 characterization included in Figure 1. All Raman spectra showed the typical F_{2g} band of
173 the ceria fluorite structure with maxima at 442-477 cm^{-1}. Note that the intensity of the
174 Raman spectra has been normalized with regard to the maximum intensity of the F_{2g}
175 band, because the fluorescence produced by praseodymium significantly affects the
176 intensity. Since the intensity is not only related to the structural order of the oxides, the
177 information about such structure is obtained from the bands position. The typical
178 position of the F_{2g} band is 464 cm^{-1} for pure ceria (dotted line in the Figure 1), and
179 zirconium doping shifts the position to higher Raman shifts while praseodymium shifts
180 the position to lower values. In accordance with the cell parameter values in Table 1, the
181 shift in the position of the F_{2g} Raman band is due to the substitution of Ce^{4+} cations by
182 smaller and larger Zr^{4+} and Pr^{3+} cations, respectively.

183 The small band or shoulder observed in the 515-600 cm^{-1} range is assigned to
184 the creation of oxygen vacancies on the oxides. The intensity of this band (after
185 normalization of the signals intensity) is highest for the ceria catalysts with highest
186 praseodymium content ($Ce_{0.5}Pr_{0.5}O_2$), in agreement with the easy reducibility of Pr^{4+} to
187 Pr^{3+}.

188 Additional information about the catalysts reducibility is obtained by H_2
189 Temperature Programmed Reduction (Figure 2). H_2 consumption is mainly attributed to
190 Ce^{4+} and Pr^{4+} reduction, because Zr^{4+} cannot be reduced under these conditions, and as
191 a general trend, the position of the bands confirms that praseodymium doping improves
192 the ceria-based catalysts reducibility with regard to zirconium doping. For all

compositions compared, the reducibility of the oxides prepared by coprecipitation is higher to that of the counterpart oxides prepared by microemulsion.

3.2. Catalytic tests.

Figure 3 shows the soot conversion curves obtained with several representative catalysts in gas mixtures with NOx + O_2 + N_2 (Figure 3a) and O_2 + N_2 (Figure 3b). For the sake of brevity, not all catalysts prepared and evaluated in this study have been included in Figure 3, but all curves can be found in the Supplementary Information (Figure 1SI). Figure 3 includes the soot conversion curves obtained with the most active catalyst prepared ($Ce_{0.5}Pr_{0.5}O_2$ (microemulsion)) together with reference curves obtained with a commercial Pt/Al_2O_3 catalyst, a $Ce_{0.5}Pr_{0.5}O_2$ catalyst prepared by a conventional coprecipitation method and the uncatalyzed curve.

The catalyst referred to as $Ce_{0.5}Pr_{0.5}O_2$ (microemulsion) is more active than the reference Pt/Al_2O_3 catalyst, being the most active soot combustion catalyst ever reported among those tested under realistic conditions (presence of NOx and poor soot-catalyst contact) if catalysts forming highly volatile species are ruled out. The $Ce_{0.5}Pr_{0.5}O_2$ (microemulsion) catalyst also has the highest surface area and the smallest particle size ever reported (125 m^2/g and 7 nm respectively) for this material. Representative surface areas reported by other authors for comparable materials are 35 and 20 m^2/g for $Ce_{0.8}Pr_{0.2}O_2$ and $Ce_{0.5}Pr_{0.5}O_2$, respectively, prepared by ammonia coprecipitation [21], 40 m^2/g for $Ce_{0.8}Pr_{0.2}O_2$ also prepared by ammonia coprecipitation [22], 48 m^2/g for $Ce_{0.8}Pr_{0.2}O_2$ prepared by microwave-assisted solution combustion [23], and 92 m^2/g for $Ce_{0.8}Pr_{0.2}O_2$ prepared by citrate precipitation [24]. As far as we know, the highest surface area ever reported for a Ce-Pr mixed oxide is 150 m^2/g for $Ce_{0.9}Pr_{0.1}O_2$ prepared by surfactant-assisted hydrothermal treatment, but this area

decreased significantly for mixed oxides with higher praseodymium concentration (90 m^2/g for $Ce_{0.5}Pr_{0.5}O_2$) [25].

For a broader comparison of the catalytic behavior, Table 2 compiles the T50% temperature, which is the temperature required to achieve 50% soot combustion, obtained in similar experiments to those shown in Figure 3a with representative catalysts of different nature. Metal oxides where the cation can hardly accomplish redox cycles (TiO_2, ZrO_2, MnO and MnO_2) show the lowest activities, followed by catalysts with non-noble transition metal cations that are able to accomplish redox cycles (Co and Cu catalysts and Mn_3O_4).

The ceria-based formulations, either with Zr or Pr dopants, present high catalytic activity, but only the Ce-Pr mixed oxides prepared in the current study by the microemulsion method are able to outperform the behavior of the platinum catalysts.

The mechanistic arguments to explain the high catalytic activity of the $Ce_xPr_{1-x}O_2$ (x = 0.8 or 0.5) mixed oxides prepared in this study by the microemulsion method have been analyzed and relevant information is obtained from combustion experiments performed in the $O_2 + N_2$ gas mixture (Figure 3b). The activity of the platinum catalyst is very low in the absence of NOx, because this catalyst mainly accelerates soot combustion by the NO_2-assisted mechanism, that is, oxidizes NO to NO_2 and NO_2 initiates soot combustion, as previously described. This is supported by the NO_2 profiles obtained in the absence of soot, which are included in Figure 4, where the highest NO oxidation capacity of the platinum catalyst is clearly evidenced. Therefore, if NOx is not available, the NO_2-assisted soot combustion mechanism is not feasible.

On the contrary (see Figure 3b), the ceria-based catalysts present significant soot combustion activity even in the absence of NOx (and the most active catalyst is

241 $Ce_{0.5}Pr_{0.5}O_2$ (microemulsion)) due to the important participation of the active oxygen-
242 based mechanism, that is, ceria catalysts exchange oxygen with the O_2 molecules and
243 deliver highly reactive oxygen species to soot [17]. Additionally, in spite of ceria
244 catalysts being less active than platinum for NO oxidation (see Figure 4), they are also
245 able to promote NO_2 formation in a certain extent, and therefore both the active oxygen
246 and NO_2-assisted mechanisms contribute simultaneously (and synergistically) to soot
247 combustion. That is why the soot combustion activity of the ceria catalysts is higher in
248 the NOx + O_2 + N_2 gas mixture (Figure 3a) than in O_2 + N_2 (Figure 3b).

249 These soot combustion experiments performed with NOx + O_2 + N_2 (Figure 3a)
250 and O_2 + N_2 (Figure 3b) gas mixtures, and the NO_2 profiles obtained in similar
251 experiments performed without soot (Figure 4), have demonstrated the important role of
252 the active oxygen mechanism in the ceria-catalyzed combustion of soot, but this was in
253 somehow already known, and additional information is required to explain the best
254 performance of the $Ce_{0.5}Pr_{0.5}O_2$ (microemulsion) catalyst.

255 As previously mentioned, the active oxygen species are unstable and will
256 recombine to each other yielding O_2 if they do not reach the carbon surface. For this
257 reason, the size of the ceria-based catalysts particles plays a key role in the combustion
258 of soot, since the lower the ceria particle size, the higher the number of contact points
259 with soot and the easier the active oxygen transfer from ceria to soot. This concept is
260 evidenced in Figure 5, where the T50% temperature obtained in soot combustion
261 experiments performed in a NOx + O_2 + N_2 gas mixture is plotted against the particle
262 size of two series of ceria-based catalysts. The ceria catalyst formulations selected are
263 the most active for Ce-Zr mixed oxide catalysts (with 20 molar % zirconium) [19] and
264 Ce-Pr mixed oxides catalysts (with 50 molar % praseodymium) [14], according to
265 previous studies. The different catalysts of each composition have been prepared

following different synthesis procedures (calcination of a physical mixture of nitrates, coprecipitation, and reverse microemulsion) and a commercial Ce-Zr mixed oxide calcined at 500 and 800 ºC has been also included.

Figure 5 shows that the Ce-Pr mixed oxides are more active than the Ce-Zr mixed oxides, and linear relationships between the particle size of the catalysts and the combustion of soot were obtained for each catalyst composition, the lower the ceria size the lower the soot combustion temperature. Each formulation follows a different linear trend because the composition determines the intrinsic activity of the mixed oxide (the active oxygen production) and the particle size the transfer of such active oxygen to soot.

Eighteen $Ce_{0.76}Zr_{0.24}O_2$ soot combustion catalysts were prepared by different methods in a previous study, and the main soot combustion mechanism was based on the catalytic oxidation of NO for most catalysts [30]. In that case, a relationship between catalyst surface area and soot combustion was found for BET areas lower than 90 m^2/g. However, the increase of the surface area above this threshold had not an additional benefit on soot combustion, and it was concluded that T50% temperatures below 490 ºC cannot be obtained with these Ce-Zr catalysts. The Ce-Pr mixed oxide nanoparticles prepared in the current study are able to obtain T50% temperatures below 490 ºC because of the relevant contribution of the active oxygen-assisted soot combustion mechanism.

As a summary, it can be concluded that both the ceria-based catalyst composition (nature and amount of dopant) and the particle size play key roles in the combustion of soot. The composition determines the production of active oxygen and the particle size the transfer of active oxygen from catalyst to soot. The optimization of

both parameters (composition of the ceria-based catalyst and size of the particles) has allowed us to prepare soot combustion catalysts that outperform the behavior of platinum-catalysts even under NOx-containing gas mixtures where commercial platinum catalysts are usually the most active ones.

4.- Conclusions.

A $Ce_{0.5}Pr_{0.5}O_2$ mixed oxide has been prepared with the highest surface area and smallest particle size ever reported (125 m^2/g and 7 nm respectively), being also the most active diesel soot combustion catalyst ever reported among those tested under realistic conditions if catalysts forming highly volatile species are ruled out. Both the ceria-based catalyst composition (nature and amount of dopant) and the particle size play key roles in the combustion of soot. The composition determines the production of active oxygen and the particle size the transfer of active oxygen from catalyst to soot. The optimization of both parameters (composition of the ceria-based catalyst and size of the particles) has allowed preparing soot combustion catalysts that outperform the behavior of platinum-catalysts even under NOx-containing gas mixtures where commercial platinum catalysts are usually the most active ones.

Acknowledgments

The authors thank the financial support of Generalitat Valenciana (Project PROMETEOII/2014/010), the Spanish Ministry of Economy and Competitiveness (Project CTQ2012-30703), and the UE (FEDER funding).

References

[1] M. V. Twigg, Appl. Catal. B 70 (2007) 2-15.

[2] B. Frank, M. E. Schuster, R. Schlogl, D. S. Su, Angew. Chem. Int. Ed. 52 (2013) 2673 – 267.

[3] R. A. Kerr, Science 339 (2013) 382.

[4] J. Tollefson, Nature 493 (2013) 454.

[5] B.A.A.L.Van Setten, M. Makkee, J.A. Moulijn, Catal. Rev. Sci. Eng. 43 (2001) 489-564.

[6] D. Fino, V. Specchia, Powd. Technol. 180 (2008) 64-73.

[7] A. Setiabudi, N.K. Allaart, M. Makkee, J. A. Moulijn, Appl. Catal. B 60 (2005) 233-243.

[8] G. Mul, J.P. Neeft, F. Kapteijn, M. Makkee, J.A. Moulijn, Appl. Catal. B 6 (1995) 339-352.

[9] K. Villani, C. E. A. Kirschhock, D. Liang, G. Van Tendeloo, J. A. Martens, Angew. Chem. Int. Ed. 45 (2006) 3106 –3109.

[10] H.S. Gandhi, G.W. Graham, R.W. McCabe, J. Catal. 216 (2003) 433–442.

[11] B.J. Cooper, H.J. Jung, J.E. Thoss (Johnson Matthey) US Patent 1999, request number US07/193,529; publication number US4902487 A.

[12] K. Krishna, A. Bueno-López, M. Makkee, J.A. Moulijn, Appl. Catal. B 75 (2007) 210–220.

[13] E. Aneggi, C. de Leitenburg, G. Dolcetti, A. Trovarelli, Catal. Today 114 (2006) 40-47.

[14] M.L. Pisarello, V. Milt, M.A. Peralta, C.A. Querini, E.E. Miró, Catal. Today 75 (2002) 465-470.

[15] L. Katta, P. Sudarsanam, G. Thrimurthulu, B.M. Reddy, Appl. Catal. B 101 (2010) 101-108.

[16] E. Kockrick, C. Schrage, A. Grigas, D. Geiger, S. Kaskel J. Sol. State Chem. 181 (2008) 1614–1620.

[17] N. Guillén-Hurtado, A. García-García, A. Bueno-López. J. Catal. 299 (2013) 181–187.

[18] B.A.A.L. Van Setten, J.M. Schouten, M. Makkee, J.A. Moulijn, Appl. Catal. B 28 (2000) 253-257.

[19] I. Atribak, A. Bueno-López, A. García-García, J. Catal. 259 (2008) 123–132.

[20] N. Guillén-Hurtado, I. Atribak, A. Bueno-López, A. García-García. J Molec. Catal. A 323 (2010) 52–58

[21] S. Imamura, J.-ichi Tadani, Y. Saito, Y. Okamotoa, H. Jindai, C. Kaito, Appl. Catal. A 201 (2000) 121–127.

[22] S. Bernal, G. Blanco, M. A. Cauqui, A. Martín, J. M. Pintado, A. Galtayries, R. Sporken, Surf. Interface Anal. 30 (2000) 85–89.

[23] L. H. Reddy, G. K. Reddy, D. Devaiah, B. M. Reddy, Appl. Catal. A 445 (2012) 297–305.

[24] G.-Q. Xie, M.-F. Luo, M. He, P. Fang, J.-M. Ma, Y.-F. Ying, Z.-L. Yan. J. Nanopar. Res. 9 (2007) 471–478.

[25] S. Somacescu, V. Parvulescu, J. M. Calderon-Moreno, S.-H. Suh, P. Osiceanu, B.-L. Su, J. Nanopart. Res. 14 (2012) 885-902.

[26] I. Atribak, I. Such-Basáñez, A. Bueno-López, A. García-García, J. Catal. 250 (2007) 75–84.

[27] I. Atribak, A. Bueno-López, A. García-García, P. Navarro, D. Frías, M. Montes, Appl. Catal. B 93 (2010) 267–273.

[28] M. Zawadzki, W. Walerczyk, F.E. López-Suárez, M.J. Illán-Gómez, A. Bueno-López, Catal. Commun. 12 (2011) 1238–1241.

[29] T. Sánchez, F.B. Gebretsadik, P. Salagre, Y. Cesteros, N. Guillén-Hurtado, A. García-García, A. Bueno-López, Appl. Clay Sci. 77-78 (2013) 40–45.

[30] I. Atribak, A. Bueno-Lopez, A. Garcia-Garcia, Top. Catal. 52 (2009) 2088–2091.

[31] I. Atribak, A. Bueno-López, A. García-García, J. Catal. 259 (2008) 123–132.

Figure Captions

Figure 1. Raman spectra of representative ceria-based catalysts calcined at 500 ºC.

Figure 2. Temperature Programmed Reduction with H_2 of ceria-based catalysts calcined at 500ºC.

Figure 3. Soot combustion curves in NOx + O_2 + N_2 (a) and O_2 + N_2 (b) either uncatalysed or with home-made $Ce_{0.5}Pr_{0.5}O_2$ and commercial platinum catalysts.

Figure 4. NO_2 production by catalytic oxidation of NO in a NOx + O_2 + N_2 gas mixture.

Figure 5. Relationship between soot combustion capacity in a NOx + O_2 + N_2 gas mixture and particle size/surface area of ceria-based catalysts. All catalysts were calcined at 500 ºC, otherwise indicated.

Table 1. Details about catalysts preparation and characterization.

Catalyst composition	Preparation method[a]	T50%[b] (ºC)	Cell parameter (nm)	BET (m^2/g)	Particle size (nm)
$Ce_{0.8}Zr_{0.2}O_2$	Microemulsion	484	0.5366	145	6
$Ce_{0.8}Zr_{0.2}O_2$	Coprecipitation	502	0.5369	57	15
$Ce_{0.8}Zr_{0.2}O_2$	Commercial	491	0.5333	113	7
$Ce_{0.8}Zr_{0.2}O_2$	Commercial (800ºC)	516	0.5351	48	18
$Ce_{0.5}Pr_{0.5}O_2$	Microemulsion	444	0.5446	125	7
$Ce_{0.5}Pr_{0.5}O_2$	Coprecipitation	485	0.5433	27	31
$Ce_{0.5}Pr_{0.5}O_2$	Nitrates calcination	477	0.5424	37	23
$Ce_{0.8}Pr_{0.2}O_2$	Microemulsion	459	0.5424	120	7
$Ce_{0.8}Pr_{0.2}O_2$	Coprecipitation	502	0.5424	70	12

[a] The catalysts were calcined at 500 ºC, otherwise indicated.
[b] Temperature required to achieve 50% soot combustion in experiments performed with a 500 ppm NOx + 5 O_2 + N_2 mixture.

Table 2. Comparison of diesel soot combustion catalysts of different nature tested in realistic laboratory conditions ("loose" soot-catalyst contact and NOx + O_2 + N_2 gas mixture).

Catalyst	T50% (ºC) [a]	Reference
No catalyst	607	[This article, 26, 27]
MnO	601	[27]
MnO_2	597	[27]
ZrO_2	592	[26]
TiO_2	593	[62]
$CoAl_2O_4$ spinel	563	[28]
Cu/hectorite	560	[29]
Mn_3O_4	510	[27]
$Ce_{0.8}Pr_{0.2}O_2$ (coprecipitation)	502	[This article]
$Ce_{0.8}Zr_{0.2}O_2$ (commercial)	488	[30, 21]
$Ce_{0.8}Zr_{0.2}O_2$ (microemulsion)	484	[This article]
$Ce_{0.5}Pr_{0.5}O_2$ (coprecipitation)	484	[This article]
Cryptomelane	481	[27]
1% Pt/$CoAl_2O_4$	478	[28]
1% Pt/Al_2O_3 (commercial)	475	[This article]
$Ce_{0.8}Pr_{0.2}O_2$ (microemulsion)	459	[This article]
$Ce_{0.5}Pr_{0.5}O_2$ (microemulsion)	444	[This article]

[a] T50% is the temperature required to achieve 50% soot combustion, the lower the better. According to reproducibility experiments, the error in the estimation of the T50% temperature is ± 2 ºC.

Figure 1

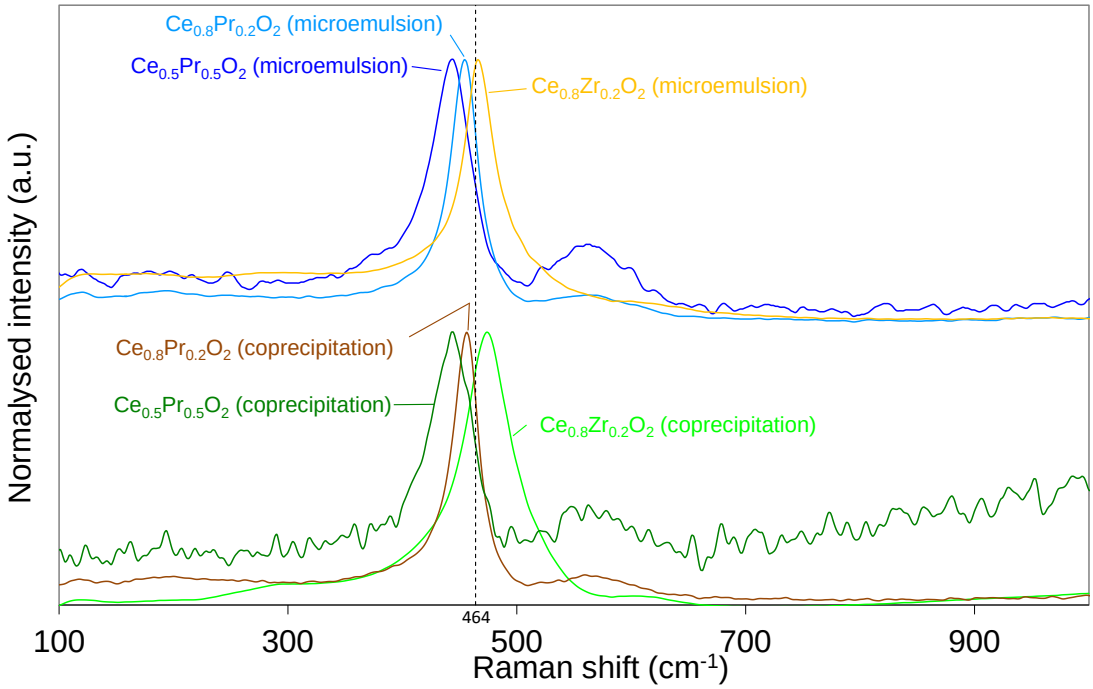
Ce0.8Pr0.2O2 (microemulsion)
Ce0.5Pr0.5O2 (microemulsion)
Ce0.8Zr0.2O2 (microemulsion)
Ce0.8Pr0.2O2 (coprecipitation)
Ce0.5Pr0.5O2 (coprecipitation)
Ce0.8Zr0.2O2 (coprecipitation)
Normalysed intensity (a.u.)
464
100
300
500
700
900
Raman shift (cm-1)

412

413 # Figure 2

414

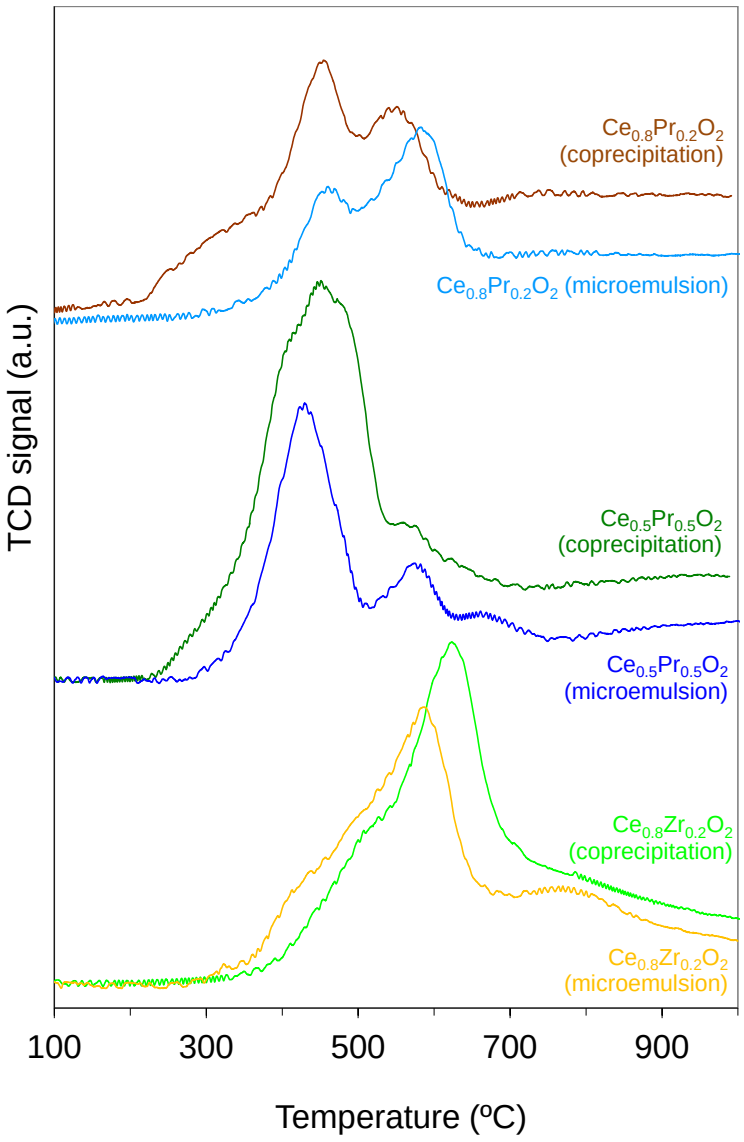

415
416

417

Figure 3

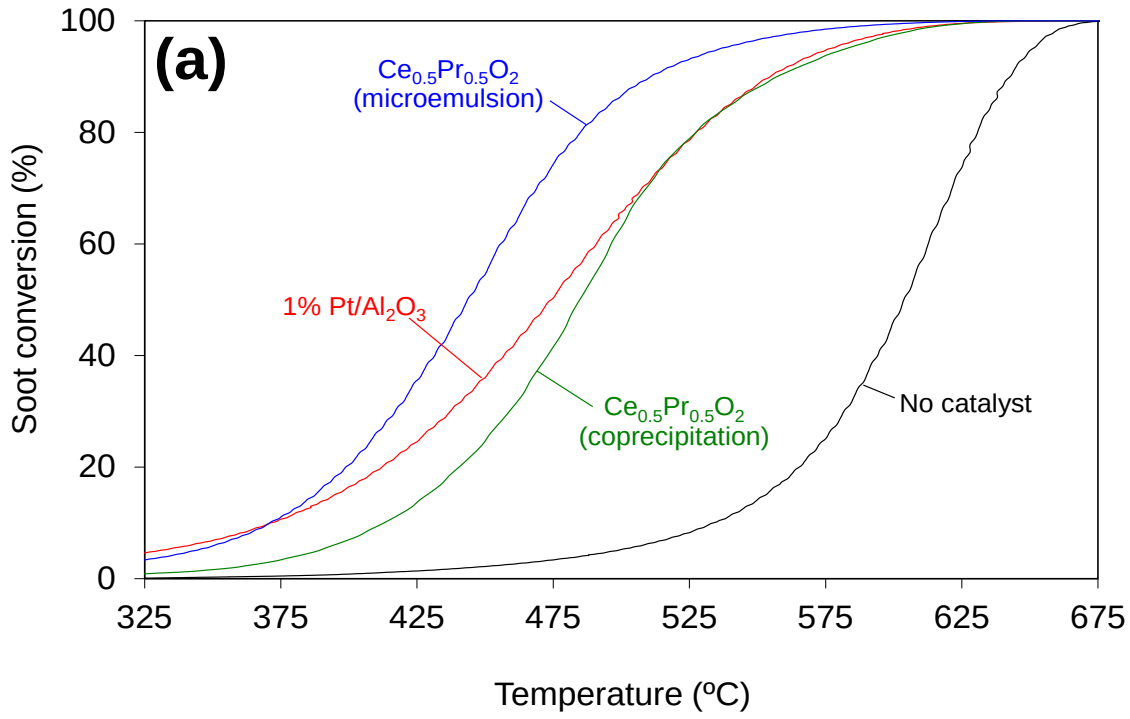
(a)
Ce0.5Pr0.5O2
(microemulsion)
1% Pt/Al2O3
Ce0.5Pr0.5O2
(coprecipitation)
No catalyst
Soot conversion (%)
Temperature (ºC)
0
20
40
60
80
100
325
375
425
475
525
575
625
675

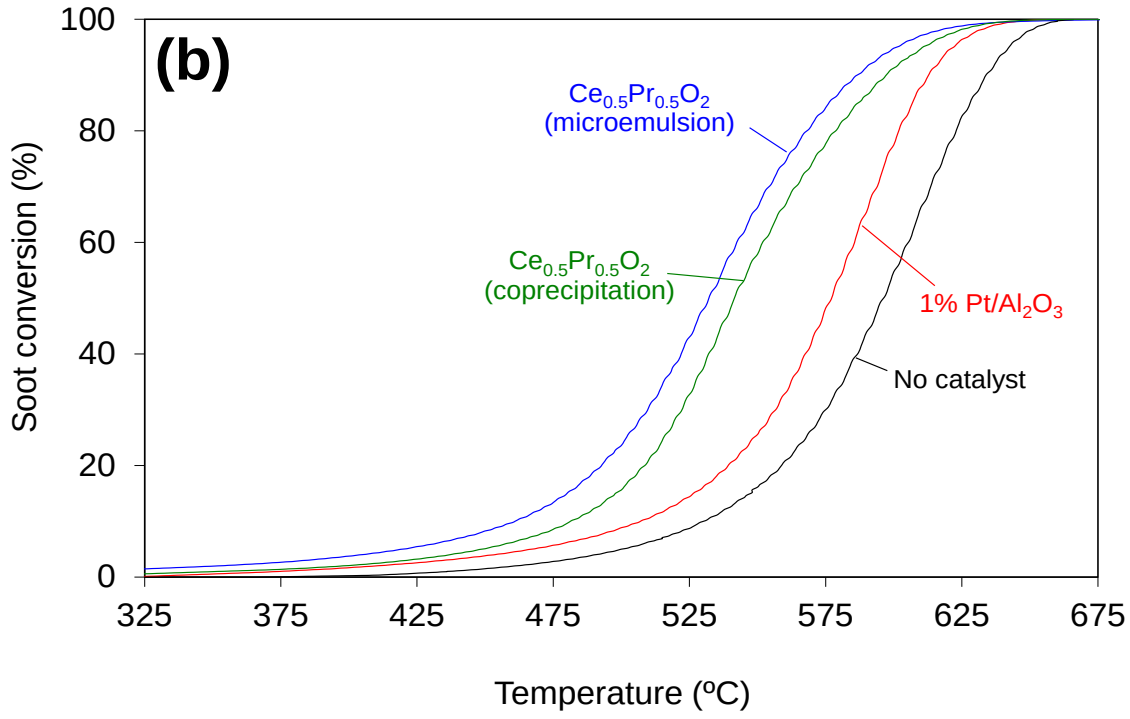
(b)
Ce0.5Pr0.5O2
(microemulsion)
Ce0.5Pr0.5O2
(coprecipitation)
1% Pt/Al2O3
No catalyst
Soot conversion (%)
Temperature (ºC)
0
20
40
60
80
100
325
375
425
475
525
575
625
675

Figure 4

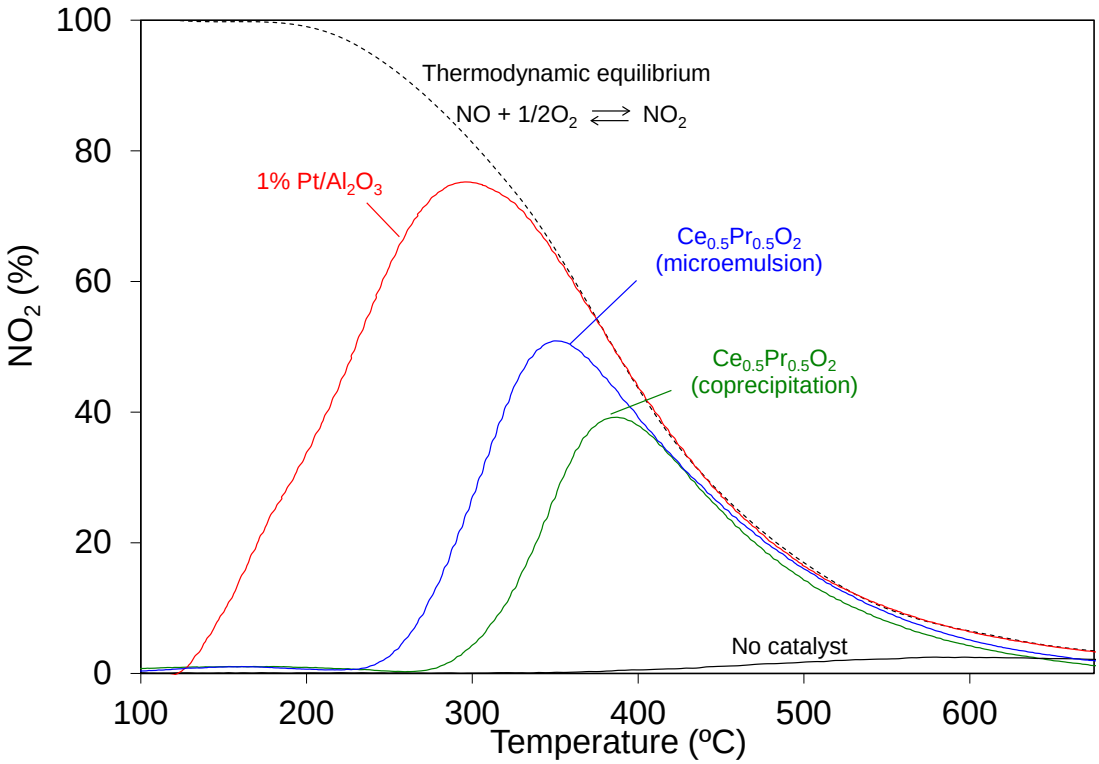
100
80
60
40
20
0
NO2 (%)
100
200
300
400
500
600
Temperature (ºC)
Thermodynamic equilibrium
NO + 1/2O2 ⇌ NO2
1% Pt/Al2O3
Ce0.5Pr0.5O2
(microemulsion)
Ce0.5Pr0.5O2
(coprecipitation)
No catalyst

Figure 5

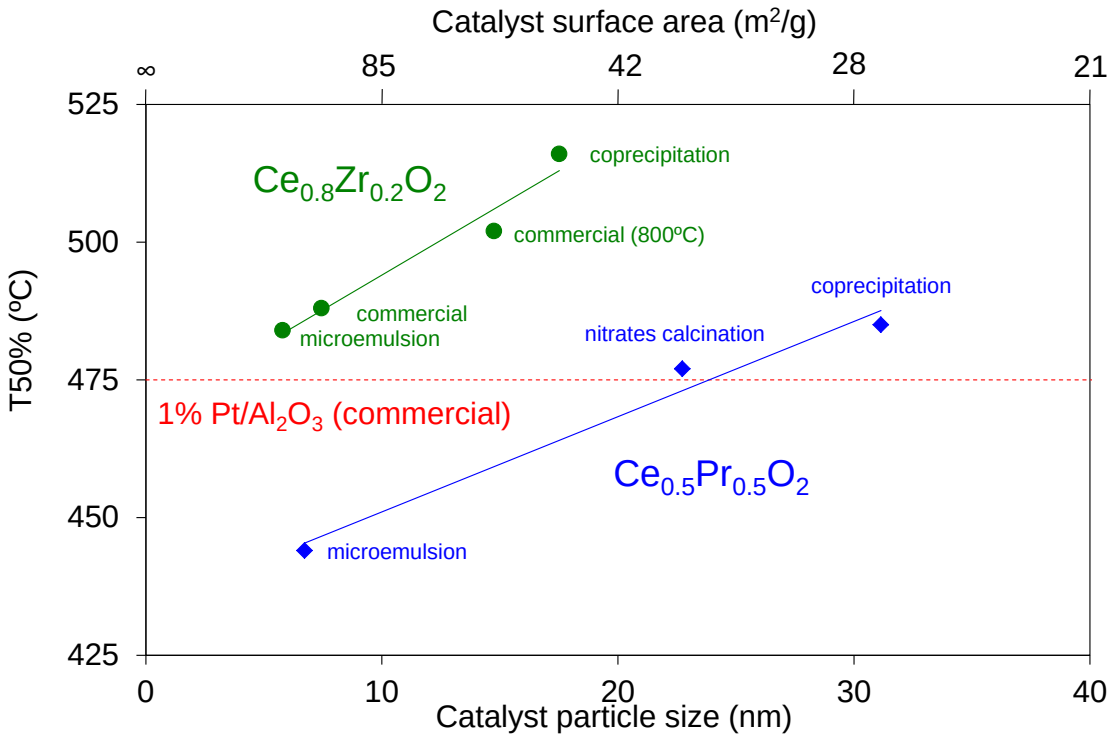
Catalyst surface area (m²/g)
∞
85
42
28
21
525
500
475
450
425
T50% (ºC)
0
10
20
30
40
Catalyst particle size (nm)
Ce0.8Zr0.2O2
coprecipitation
commercial (800ºC)
commercial
microemulsion
1% Pt/Al2O3 (commercial)
coprecipitation
nitrates calcination
Ce0.5Pr0.5O2
microemulsion